Bonding in minerals: the application of PAX (photoelectron and X-ray) spectroscopy to the direct determination of electronic structure

DAVID S. URCH

Chemistry Department, Queen Mary College, Mile End Road, London E1 4NS, UK

Abstract

X-ray photoelectron spectroscopy can be used to measure the ionization energies of electrons in both valence band and core orbitals. As core vacancies are the initial states for X-ray emission, a knowledge of their energies for all atoms in a mineral enables all the X-ray spectra to be placed on a common energy scale. X-ray spectra are atom specific and are governed by the dipole selection rule. Thus the individual bonding roles of the different atoms are revealed by the fine structure of valence X-ray peaks (i.e. peaks which result from electron transitions between valence band orbitals and core vacancies). The juxtaposition of such spectra enables the composition of the molecular orbitals that make up the chemical bonds of a mineral to be determined.

Examples of this approach to the direct determination of electronic structure are given for silica, forsterite, brucite, and pyrite. Multi-electron effects and developments involving anisotropic X-ray emission from single crystals are also discussed.

KEYWORDS: X-ray emission spectroscopy, X-ray photoelectron spectroscopy, electronic structure.

Introduction

THE bombardment of minerals with reasonably energetic (>100 eV) photons (X-rays), or electrons or other charged particles creates vacancies in core atomic orbitals which can relax either by X-ray emission or by the ejection of an Auger electron. In either case the energy of the photon or electron is characteristic of the atom from which it came. For this reason both X-ray emission (XE) spectroscopy and Auger-electron (AE) spectroscopy are widely used for elemental analysis; XE for the bulk analysis of solids (Herglotz and Birks, 1978) and AE for the analysis of surfaces (Briggs and Seah, 1983). If, however, the electronic transition involves the valence band, then both types of spectra [Valence X-ray Emission (VXE) spectra and Valence Auger Electron (VAE) spectra] can give rise to complex peaks which reflect (in part) the band structure of the sample, be it metal or alloy, chemical compound, transition metal complex, or mineral. VAE spectra, because the final states are doubly ionized, are quite complex and do not lend themselves to such simple interpretation as the corresponding X-ray spectra. For this reason only VXE spectra will be considered in this paper.

X-ray emission spectroscopy. The basic principles of an X-ray emission spectrometer, in which X-ray spectra including VXE spectra can be measured, are well known (see, for example, Compton and Allinson, 1935; Agarwal, 1979; or Jenkins and de Vries, 1970). X-ray emission, except for hard X-rays with short wavelengths ($\lambda < 2$ Å), is governed by the electric dipole selection rule (Laporte Rule), which requires that the atomic orbital angular momentum quantum number should change by one, $\Delta l = \pm 1$.

Thus X-rays will only be observed as a result of a transition to an *s* vacancy on atom A from *p* orbitals of atom A or orbitals with A *p* character. Similarly transitions to an A *p* vacancy will only arise from orbitals with A *s* or A *d* character and A *p* and A *f* are the only types of orbital that could initiate a transition to an A *d* vacancy. This results in a considerable simplification in the potential complexity of X-ray spectra. It also provides the chemist and the mineralogist with a unique probe of electronic structure. This is because molecular orbitals can participate in the X-ray emission process just as freely as atomic orbitals. If molecular orbitals (see texts such as Murrell *et al.*, 1965, for an introduction to

Mineralogical Magazine, April 1989, Vol. 53, pp. 153–64

molecular orbital theory) are regarded as linear combinations of atomic orbitals (LCAO) approximation),

$$\varphi_i = \Sigma a_{ri}\,\theta_r,$$

where a_{ri} is a coefficient which describes the contribution of atomic orbital θ_r to molecular orbital φ_i, then it can be shown (Manne, 1970) that the intensities of the peaks observed in the fine structure of a VXE peak from atom A are directly proportional to the squares of the coefficients a_{ri}: it is found that the relaxation process is localized on A and that orbitals from other atoms usually make no great direct contribution to the observed X-ray intensity (Urch, 1970; but see also Larkins and Rowlands, 1986). Thus a study of Si–$K\beta_{1,3}$ spectra provides a direct probe of the bonding role of silicon $3p$ orbitals. If Si–$L_{2,3}M$ spectra were also investigated they would enable the complimentary contributions of silicon $3s$ and silicon $3d$ orbitals to be determined.

For the structure of each molecular orbital in a mineral to be determined in this way, the spectra must be placed on a common energy scale. In the example chosen above, the silicon $K\beta$ spectrum, 1815–1840 eV, must be correctly aligned with the Si–L spectrum, 70–100 eV, so that a direct one-to-one correspondence between spectral features and molecular orbitals can be established. In this particular case, a direct measurement of the Si–$K\alpha_{1,2}$ spectrum would suffice, but in the more general situation it is necessary to compare spectra taken from a variety of different atoms. The binding energies of the molecular orbitals, E(MO), that give rise to the fine structure of a VXE peak, are given by the equation,

$$E(\text{MO}) = E(\text{initial X-ray state}) - E(\text{X-ray}).$$

Thus, when the energy of the initial vacancy state has been measured, the X-ray energy scale for each spectrum can be replaced by a molecular orbital ionization energy scale. And when this has been done for all the different X-ray spectra from a compound, all the spectra can be aligned against the common (molecular orbital) energy scale. Peaks in different spectra but which originate from the same molecular orbital can then be clearly seen to be related. The necessary measurement of initial state energies can most easily be carried out by determining core orbital ionization energies by X-ray photoelectron (XP) spectroscopy.

X-ray photoelectron spectroscopy. In XP spectroscopy the sample is bombarded with as nearly monoenergetic photons as is possible. Simple, convenient and widely used excitation sources are

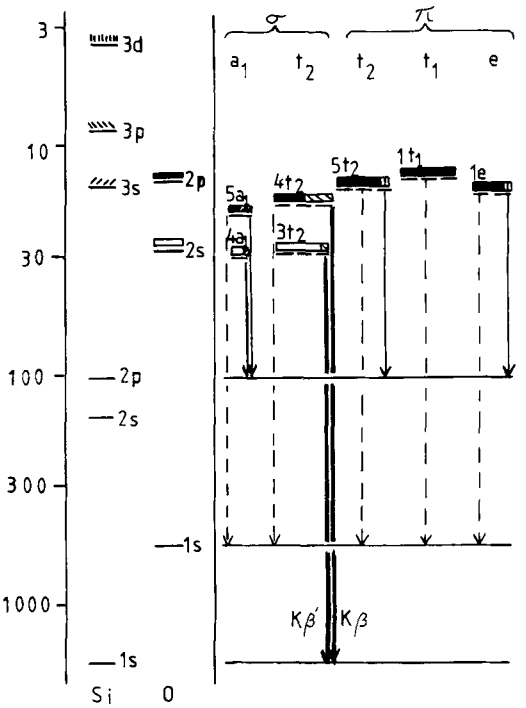

FIG. 1. Qualitative molecular orbital energy level diagram for the silicate anion. The vertical scale, in electron volts, is logarithmic. Atomic orbitals are on the left, the resulting molecular orbitals, on the right. The composition of the molecular orbitals is indicated by hatching, shading, etc. For simplicity the effect of interaction between $4t_2$ and $5t_2$ has been omitted; it would lead to some Si $3d$ character being present in $4t_2$ and some Si $3p$ character entering $5t_2$. Possible X-ray transitions are shown as dashed lines for O–$K\alpha$, solid lines for Si–$L_{2,3}M$ and heavy lines for Si–$K\beta$.

the $K\alpha$ X-rays emitted by aluminium (1486.6 eV) and magnesium (1253.6 eV). These sources have line widths of less than one electron volt which give satisfactory spectra in most cases. The kinetic energies of the photoelectrons are measured directly and the ionization energy (binding energy) of the orbital from which they came determined by the equation (ignoring recoil),

$$E_b(\text{binding energy}) = E(\text{h}\nu) - E_k(\text{photoelectron kinetic energy}),$$

where $E(\text{h}\nu)$ is the energy of the incident radiation (basic details of XP spectrometers are reviewed by Rivière, 1983). In the case of insulating solids, complications can arise due to the sample becoming charged during the experiment. This problem can be overcome either by neutralizing the charge with low energy electrons (using a 'flood gun') or by careful attention to calibration.

Table 1. Symmetry classification of silicon and oxygen valence atomic orbitals for the silicate anion $[SiO_4]^{4-}$, point group T_d.

Orbitals	Irreducible representation	Orbitals	Irreducible representation
Si 3s	a_1	O 2s	$a_1 + t_2$
Si 3p	t_2	O 2p (directed along Si-O)	$a_1 + t_2$
Si 3d	$e + t_2$	O 2p (perpendicular to Si-O)	$e + t_1 + t_2$

Because XP spectroscopy depends upon the measurement of electron energies which are only of the order of a thousand volts or less, it is a very surface-sensitive technique. The only photoelectrons that emerge from the sample with energies unattenuated by collision are those from the top five to ten atomic layers. This calls for great care in experimental technique (typical operating conditions are 10^{-9} torr), scrupulous attention to sample cleanliness and an appreciation, when interpreting the resulting spectra, of the very limited sample depth that has been probed. Attempts to 'clean' samples by heavy ion bombardment, e.g. Ar^+, unfortunately lead, not only to the removal of surface contamination, but also to chemical (Holm and Storp, 1977) and physical damage to the sample itself. Differential sputtering can distort analytical results and the reduction which bombardment causes compromises the determination of valency by consideration of 'chemical shifts' (see below).

As every atom has atomic orbitals with unique ionization energies, XP spectroscopy is widely used for the identification of the elements present on sample surfaces. It is also found that the ionization energies are subject to small perturbations (a few volts or so) which can be related to factors such as valency, ligand atom electronegativity and crystal structure. These 'chemical shifts' can, therefore, be used to determine the chemical state of an atom and sometimes the identity of the atoms to which it is bound, (a useful review of the basic features of XP spectroscopy is by Hagström and Fadley, 1974).

XP spectroscopy is not subject to such stringent selection rules as is XE spectroscopy, so that electrons from each orbital in every atom can, in principle, yield a spectral peak. There are, however, wide variations in peak intensity, governed in the main by the efficiency with which the orbital (radial) wave function overlaps with the plane wave of the ejected photoelectron (Price, 1977). This results in peaks in XP spectra corresponding to valence band electrons usually being very weak and in peaks derived from 2*s* orbitals of first row elements being relatively more intense than those derived from 2*p* orbitals (Scofield, 1976).

It can, therefore, be seen that XP spectroscopy provides basic information about the ionization energies of the molecular orbitals present in a mineral and some limited information about their structure in terms of constituent atomic orbitals. It also yields valuable information about core ionization energies from which valence states can be deduced and which can be used to assemble XE spectra. Each X-ray emission spectrum provides detailed information about the disposition of specific atomic orbital character amongst the molecular orbitals of the valence band. Alignment of such spectra from all the different atoms of a mineral thus enables a detailed picture of the atomic orbital structure of each molecular orbital to be built up. A combination of XP and XE spectra—PAX spectroscopy—thus shows clearly and directly the electronic structure of a mineral, the nature of the bonding is revealed, and the chemical bond is 'dissected'.

Molecular orbital model: the silicate anion

The application of simple molecular orbital (MO) models of electronic structure to the interpretation of PAX spectra can be exemplified by the silicate anion. The tetrahedral symmetry allows the constituent atomic orbitals to be classified according to their irreducible representations (Urch, 1979) as shown in Table 1.

The numbering of the molecular orbitals that result from the interactions of these atomic orbitals includes the core orbitals—Si 1*s*, $1a_1$—O 1*s*,

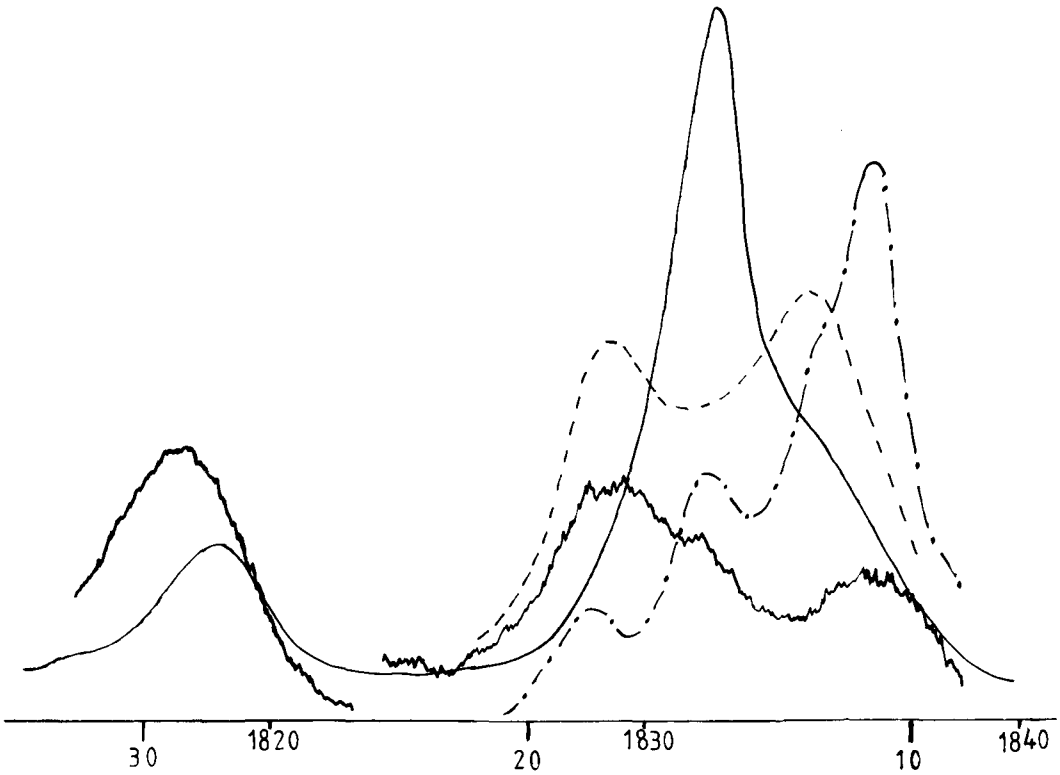

FIG. 2. PAX spectra for α-quartz. The vertical scale is in arbitrary units. The spectra are differentiated as follows: XPS, solid line showing some noise (note scale change, ×3, at 24 eV); Si–$K\beta$, smooth solid line; Si–$L_{2,3}M$, dashed line (data from Brytov *et al.*, 1976); O–$K\alpha$, dash–dot–dash line. The upper scale refers to Si–$K\beta$, the lower to the ionization energies of the valence band orbitals.

$2a_1 + 1t_2$—Si $2s$, $3a_1$—Si $2p$, $2t_2$. The calculation of the energies and of the wave functions of the MOs can be simplified if it is assumed that the oxygen $2s$ orbitals are quite tightly bound and that the oxygen $2p$ orbitals perpendicular to Si–O bonds overlap principally with Si $3d$ orbitals. The main σ interaction between silicon and oxygen orbitals then involves only Si $3s$ (a_1), Si $3p$ (t_2) and O $2p$ orbitals which are orientated towards the central silicon. This interaction will give rise to four bonding ($5a_1$ and $4t_2$) and four anti-bonding orbitals. Because the atomic orbitals transform under the same irreducible representations, some Si $3s$ and Si $3p$ character will also be found in the tightly bound orbitals that are mostly O $2s$, $4a_1$ and $3t_2$ respectively. The orbitals $1e$ and $5t_2$ are mostly, and $1t_1$ exclusively, oxygen $2p$. But as Si $3d$ orbitals transform as e and t_2, π-type interaction with such O $2p$ orbitals is possible. Furthermore, the distinction between the type of bonding engaged in by the O $2p$ orbitals directed towards silicon and those perpendicular to this direction, is based on overlap and not on symmetry, so the possibility of σ–π mixing between $4t_2$ and $5t_2$ must not be overlooked. These calculations can be summarized as a qualitative molecular orbital energy level diagram, Fig. 1.

This very simple model can now be used to rationalize the PAX spectra from the silicate anion. As it is not possible to observe such a species in isolation, silica will be used as an example in which all the silicon atoms are in identical tetrahedral environments surrounded by four oxygen atoms. Allowance will then have to be made for the fact that every oxygen atom is bridging and not singly bound to silicon.

Silica. The PAX spectra for silica (α-quartz) are shown in Fig. 2. The most tightly bound of the valence band orbitals ($4a_1$, $3t_2$) can be related to peaks at about 28–30 eV. These peaks can be shown to be mostly oxygen $2s$ by the relative intensity of the peak in the XP spectrum (O $2s$ has an Al–$K\alpha$ photoelectric cross-section about eight times larger than that for O $2p$, Scofield,

1976). The presence of some Si $3p$ character in $3t_2$ gives rise to the 'low-energy satellite', Si–$K\beta'$. The main peaks in the silicon $L_{2,3}M$ and $K\beta$ spectra at 18 and 15 eV can then be identified as reflecting Si $3s$ and Si $3p$ character in the σ bonds, $5a_1$ and $4t_2$. The presence of oxygen $2p$ character in these same orbitals is shown by corresponding peaks in the oxygen $K\alpha$ spectrum. The main peak in this spectrum is, however, to be associated with the orbitals $1e$, $1t_1$ and $5t_2$, which, by consideration of the relative intensities of the component peaks in the O–$K\alpha$ spectrum, must have considerable lone pair character. The presence of an intense feature in the silicon $L_{2,3}M$ spectrum at 12.5 eV shows (Urch, 1969) that silicon does indeed use its $3d$ orbitals in π-bond formation with oxygen (although it is not possible to quantify this effect by comparison with other peaks in the Si–L spectrum as they are associated with Si $3s$ character—unless difficult to justify assumptions are made about the relative sizes of $3s$ and $3d$ radial functions; see Taniguchi and Henke, 1976). The Si–$K\beta$ spectrum also shows evidence of a peak at about 12 eV which could be due to the presence of Si $3p$ character in $5t_2$. As the spectra are for silica this peak cannot be construed as evidence for σ–π mixing, since in silica one of the 'lone-pair' orbitals from each oxygen will be involved in σ bonding to a neighbouring silicon. Apart from this, however, the qualitative molecular orbital model (Fig. 1) provides a remarkably simple and comprehensive interpretation of the PAX spectra of silica and inspires confidence that this approach will prove adequate for the interpretation and understanding of similar spectra from other minerals. It also shows that such spectra can be related directly to electronic structure in minerals.

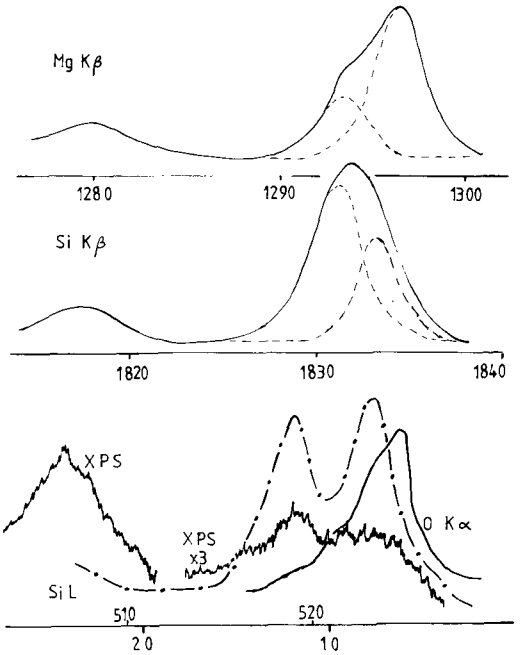

FIG. 3. PAX spectra for forsterite (data from Al-Kadier *et al.*, 1984). The lowest energy scale shows the ionization energies of the molecular orbitals determined by XPS. Probable component peaks are shown as dashed lines. In the lowest section silicon $L_{2,3}M$ is the dash–dot line (90–100 energy scale) and oxygen $K\alpha$ the solid line (510–520 energy scale).

Forsterite. The same molecular orbital model can, of course, be applied to any mineral in which the silicate unit occurs: a simple example is the orthosilicate, forsterite (Al-Kadier *et al.*, 1984). In this olivine mineral the isolated silicate tetrahedra are located in close proximity to magnesium cations so that the latter are coordinated by distorted octahedra of oxygens. The PAX spectra are shown in Fig. 3. Whilst the Si–L (but see Tossell, 1977, for a discussion of Si–L spectra from quartz and olivine) and O–$K\alpha$ are quite similar to the corresponding quartz spectra, Si–$K\beta$ is much broader. This increase in breadth can most easily be understood as due to an increase in the intensity of the component peak at 1834 eV relative to that at 1831 eV. The reason for this change is associated with the change from Si–O–Si links in silica to Si–O–Mg in forsterite. Magnesium (Mg^{2+}) being much less strongly polarizing than silicon (Si^{4+}) the oxygen 'lone-pair' orbitals (those perpendicular to Si–O) will be more available for bonding to silicon: changes in the Si–O–X bond angle may also be important in determining the relative intensities of these two Si–$K\beta$ peaks. An appreciation of the difference in polarizing power between magnesium and silicon is also necessary for the changes in $K\beta$ peaks profiles to be understood. The perturbation of the electronic structure of silicate brought about by magnesium cations will be slight, Mg–$K\beta$ will, therefore, be expected to follow, more or less, the O–$K\alpha$ peak profile since the latter indicates the availability of oxygen $2p$ electrons. The correspondence is not exact because of differences in overlap between the magnesium $3p$ orbitals and the $4t_2$ and $5t_2$ orbitals of silicate.

The application of molecular orbital theory to the interpretation of X-ray spectra of minerals was first proposed by Glenn and Dodd (1968) for absorption spectra; the method was extended to emission spectra (Dodd and Glenn, 1968*a*,*b*; Manne, 1970; Urch, 1970). Simple quantitative molecular orbital methods, Extended Hückel

(Brytov *et al.*, 1976) and CNDO/2 (Dikov *et al.*, 1977), as well as more sophisticated theoretical methods e.g. *ab initio* (Collins *et al.*, 1972 on $[SiO_4]^{4-}$ and H_4SiO_4) and the SCF $X\alpha$ scattered wave method (Tossell *et al.*, 1973 on SiO_2, Tossell, 1975 on $[SiO_4]^{4-}$), have all been used to rationalize Si–L, and Si–K peak shapes and the relative intensities of component peaks. Molecular orbital methods have also been used as a basis for understanding the VXE spectra of other elements, such as aluminium or magnesium, present in rock-forming minerals (Tossell, 1975).

Shifts in Si–$K\beta$ peak energy have been reported for many minerals (e.g. White and Gibbs, 1967) and have been correlated with changes in Si–O bond lengths and also with Si–O–X (where X is any atom but usually Si or Al) inter-bond angles. An extension of this work is reported in this volume in a companion paper (Purton and Urch, 1989). Similar shifts and correlations have also been found for silicon 2p core ionization energies for which rationalizations based on CNDO/2 calculations have been proposed (Tossell, 1973).

The various theoretical methods that have been used to interpret silicate PAX spectra have all demonstrated the value of the MO approach. Furthermore, they have demonstrated that even the simplest model (see Fig. 1) gives results that are qualitatively correct and in agreement with those from much more sophisticated calculations. Because of its simplicity and ease of application, the Hückel MO method will be used in the examples discussed below as the basis for the interpretation of PAX spectra and their use in the determination of the electronic structure of minerals.

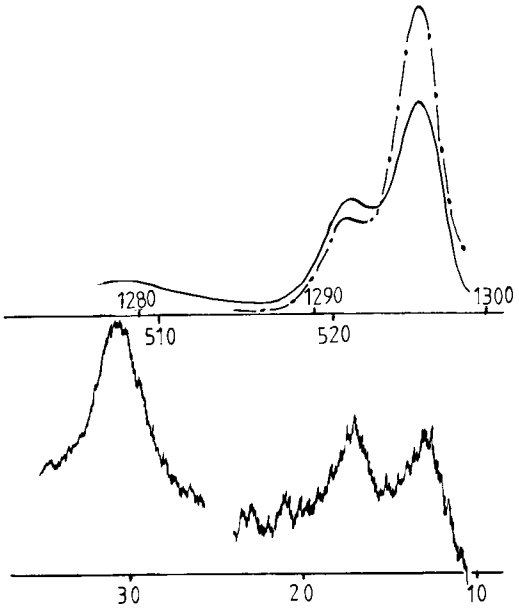

FIG. 4. PAX spectra for brucite (data from Haycock *et al.*, 1979). The upper section shows Mg–$K\beta$, solid line (1280–1290 energy scale) and O–$K\alpha$, dash–dot line (510–520 energy scale). The VXP spectrum is shown below—note scale change, ×3, at 25 eV.

Electronic structures of other minerals

The purpose of this section is to show how PAX spectra from other types of minerals can be used to investigate electronic structure. A simple hydroxide and a sulphide have been chosen as examples.

Brucite. In this mineral, layers of magnesium cations lie between layers of oxygens, present as part of hydroxyl anions. Each magnesium ion is octahedrally coordinated by oxygen and is orientated so that three oxygens lie in each of the 'oxygen' layers. Each oxygen is bound to three magnesiums and to one hydrogen. The simplest model for the bonding in brucite would be wholly ionic, $Mg^{2+}(OH)_2^-$ but this would require the Mg 3p orbitals to be quite empty and so no Mg–$K\beta$ spectrum should be observed. This is not so, as can be seen from Fig. 4 where the PAX spectra from brucite are presented. Thus, whilst the ionic model is a useful 'zero order approximation' to the electronic structure, it clearly cannot be the whole story. It is reasonable to assume that much stronger covalent bonding exists between the oxygen and the hydrogen of the hydroxyl group than between magnesium and oxygen. Detailed molecular orbital calculations have shown (Cade, 1967) that the bonding in the hydroxyl anion consists of a σ bond with considerable O 2p character, a contribution from H 1s and a few percent of O 2s character, together with two O 2p 'lone-pair' orbitals, the σ orbital being about 4 eV more tightly bound than the non-bonding orbitals. The H–O–Mg angle is such that magnesium orbitals will be able to interact with both bonding and lone-pair orbitals of hydroxyl. If this interaction is nothing more than a minor perturbation (i.e. the Mg–OH bonding remains mostly ionic) then it will not greatly alter the nature of the bonding in hydroxyl, so it is possible to describe the bonding in brucite in terms of the electronic structure of hydroxyl with the minor transfer of charge from the orbitals of hydroxyl to magnesium.

This model is in accord with the observed spectra (Haycock *et al.*, 1979). The relative intensities

and energies of the component peaks of O–$K\alpha$ at 525 and 521 eV are as expected for hydroxyl. The main peak in Mg–$K\beta$ shows a structure which aligns with the σ and 'lone-pair' peaks of O–$K\alpha$; the relative intensities can be rationalized as due to different overlap of the Mg 3*p* orbitals with the two oxygen orbitals. The low-energy satellite, Mg $K\beta'$ (1278 eV), can be understood, as in the case of silicate, as arising from Mg 3*p* character in orbitals that are mostly O 2*s*. A strange feature of the PAX spectra is the almost equal intensity observed for the two peaks at 13 and 17 eV in the XP spectrum. If, indeed, most of the electronic charge in the valence band of brucite does reside near to the oxygen atoms, then this part of the XP spectrum should resemble the O–$K\alpha$ XE spectrum, two peaks of relative intensity 1:3, not more nearly 1:1. The most plausible explanation is to be found in the small percentage of O 2*s* character that is present in the bonding orbital which gives rise to the peaks at 17 eV (521 O–$K\alpha$, 1292 Mg–$K\beta$). Whilst the presence of O 2*s* could in no way affect the O–$K\alpha$ spectrum it could significantly augment the intensity of an XP peak as the O 2*s* photoelectron cross-section is much greater than that for O 2*p*. Thus, all the brucite PAX spectra accord with a model of the electronic structure that proposes a strong covalent bond between oxygen and hydrogen in hydroxyl and a mostly ionic bond, but with some covalent character, between oxygen and magnesium.

Pyrite. In pyrite Fe^{2+} and S_2^{2-} ions are arranged in a halite-type lattice. The centre of the disulphide unit replaces the chloride anion and the coordination about each sulphur atom is roughly tetrahedral, three irons and one sulphur. Many attempts have been made to relate pyrite PAX spectra to calculated electronic band structures (Wiech *et al.*, 1972; Li *et al.*, 1974; Sugiura *et al.*, 1976; Berg *et al.*, 1976). Most discussions have either concentrated on the FeS_6 unit or the S_2 unit and neither approach has provided a wholly satisfactory picture. The PAX spectra are shown in Fig. 5. The least tightly bound orbitals, at 1.5 eV, give rise to the main peak in Fe–$L\alpha$ and so are to be associated with Fe 3*d* character. The diamagnetic nature of pyrite requires the absence of unpaired electrons so that if a wholly ionic model were postulated then there should be a single sharp Fe–$L\alpha$ peak for Fe $3d^6$ (t_{2g}). The presence of additional structure, in both the Fe–$L\alpha$ and in the S–$K\beta$ spectra shows that the simple ionic model cannot be true. Fe–$K\beta_{2,5}$ (which reflects Fe 4*p* character) and Fe–$L\alpha$ both overlap S–$K\beta$ indicating the presence of molecular orbitals with both iron 4*p* or 3*d* and S 3*p* character. Even so, the ionic model provides a convenient

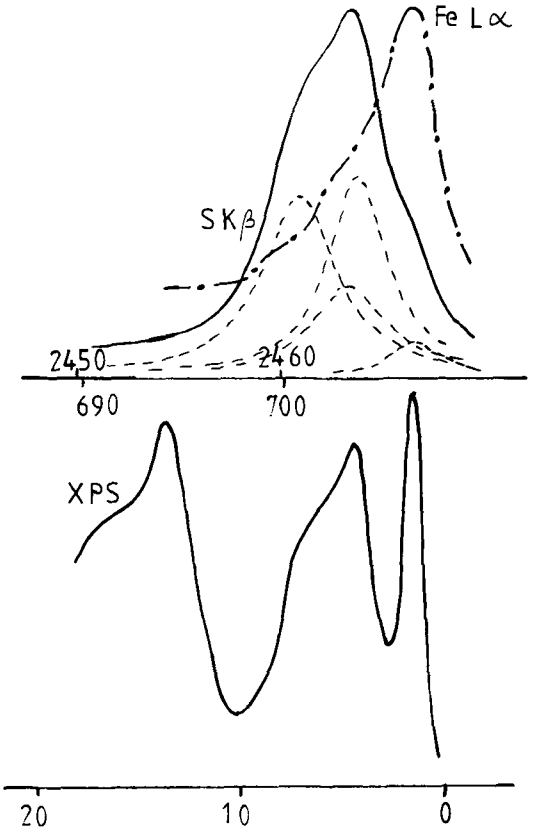

FIG. 5. PAX spectra for pyrite. Upper section shows S–$K\beta$ as a solid line with component peaks as dashed lines and the Fe–$L\alpha_{1,2}$ spectrum as a dash–dot line. The energy scales are, 2450–2460 S–$K\beta$ and 690–700 Fe–$L\alpha$. The VXP spectrum is in the lower section.

starting point for the construction of a model to describe the bonding in pyrite.

The disulphide dianion will be expected to have an electronic structure,

$$\sigma_g^2(3s) \quad \sigma_u^2(3s) \quad \sigma_g^2(3p) \quad \pi_u^4(3p) \quad \pi_g^4(3p)$$

with some mixing of 3*s* and 3*p* character between $\sigma_g(3s)$ and $\sigma_g(3p)$. If the ordering of the orbitals also indicates their relative energies (most tightly bound first, least tightly bound last) then it is most difficult to understand the S–$K\beta$ peak profile (Urch, 1985). Reasonable agreement can, however, be obtained if $\pi_u(3p)$ is considered to be more tightly bound than $\sigma_g(3p)$: the inversion of the anticipated order may be due to $\sigma_g(3s)$, $\sigma_g(3p)$ mixing referred to above (a similar inversion has been observed for N_2; Siegbahn *et al.*, 1969). The other structure observed in S–$K\beta$ at 2467 eV and which aligns with the main Fe–$L\alpha$ peak is due

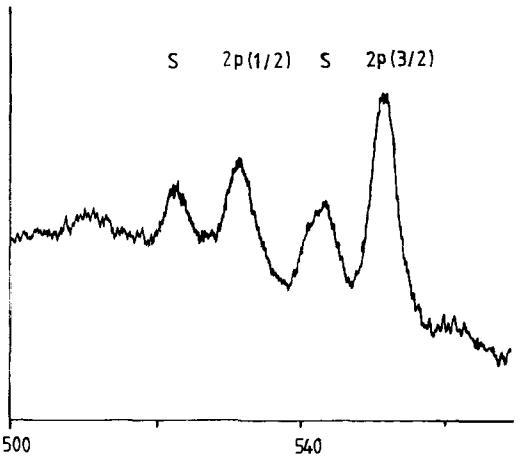

FIG. 6. Copper(II) oxide XP spectrum for the Cu $2p$ region. Energy scale is the kinetic energy of the photoelectron. 'Shake-up' satellite peaks are indicated by S. (Such peaks are absent from Cu(I) spectra).

to covalent bond formation between iron $3d$ orbitals and the antibonding π orbitals of S_2^{2-}. Such covalent interaction between two filled orbitals must result in two new bands of molecular orbitals, evidence for the other set is to be found in the structure on the low energy side of the Fe–$L\alpha$ X-ray peak at 703 eV, overlapping the main S–$K\beta$ peak. This model thus provides a qualitative rationalization for the main features in the PAX spectra and enables the presence of covalent bonding between iron and sulphur in pyrite to be established.

Many-electron effects in PAX spectra of minerals

The discussion of XE and PE spectra presented above has been based on the 'one-electron, frozen-orbital' approximation in which it is assumed that the electron transitions and ionization processes which lead to X-ray emission and to the ejection of photoelectrons can be described by considering just the one electron directly involved. The other electrons in the atom or the molecule remain indifferent, unperturbed by the violent change. Of course, this is not so (Martin and Shirley, 1977) and some of the effects wrought by the involvement of all electrons in the generation of XE and XP spectra will be described below.

Shake-up, shake-off, configuration interaction. Whilst MO one-electron models for ground and excited states are often remarkably accurate, they can be improved by allowing other excited states (of the correct symmetry) to interact with the initial state. This means that many different configurations can be found contributing, in varying degrees, to the final wavefunction for any one particular state (see, for example, Atkins, 1983). This effect is particularly evident in some XP transition metal spectra. Thus the $2p^{-1}$ configuration of Cu(II) interacts not only with the ground state $(t_{2g})^6\ (e_g)^3$ configuration but also with the excited state $(t_{2g})^5\ (e_g)^4$ so that two peaks are observed for '$2p^{-1}$' (see Fig. 6 and Frost *et al.*, 1972). As this could also be regarded as due to $2p$ photoionization with, sometimes, simultaneous $3d$ excitation, the formation of an extra peak of lower kinetic energy than the main peak is often called a 'shake-up' satellite (Krause and Carlson, 1967). In principle, many such peaks are possible and under conditions of high resolution can often be observed: when excitation reaches the limit of ionization the satellite is termed 'shake-off'. Cases are also known where these configuration interaction effects can cause such large perturbations that peaks are no longer found where the one electron model would predict them. A classic case is that of the non-existent Xe $4p$ peak (Wendin and Ohno, 1976) but examples can also be found in valence band spectra (e.g. '$3s$' peaks in both XP and XE spectra from P, S, etc., are often both split and displaced by many volts from their anticipated 'one-electron' positions—Domcke *et al.*, 1978).

High-energy satellites in XE spectra. When multiply-ionized ions relax, X-rays or Auger electrons are emitted. In the former case the energies are usually a little larger than for the corresponding X-rays emitted in a singly ionized system. The presence of more than one vacancy in the electronic structure of the emitting atom leads, by spin-orbit coupling, to many possible spectroscopic states of different energies, which can be involved in the X-ray emission process. High-energy satellites of this type, therefore, show considerable fine structure. Even spectrometers with modest resolving power can distinguish $K\alpha'$, $K\alpha_3$ and $K\alpha_4$ from the light elements such as fluorine (Urch, 1982). These satellite peaks, even when due to core-to-core transitions, often show chemical effects such as changes in relative intensity and changes in overall intensity relative to the main, diagramme line, peak (Läuger, 1972; Fischer and Baun, 1965). The reasons for these changes are poorly understood. By way of example some Si–$K\alpha_{3,4}$ peaks for different silicon compounds are shown in Fig. 7 (after Purton, pers. comm.).

Exchange coupling. In open-shell systems such as transition metal complexes or minerals containing transition metal ions, exchange and spin-orbit

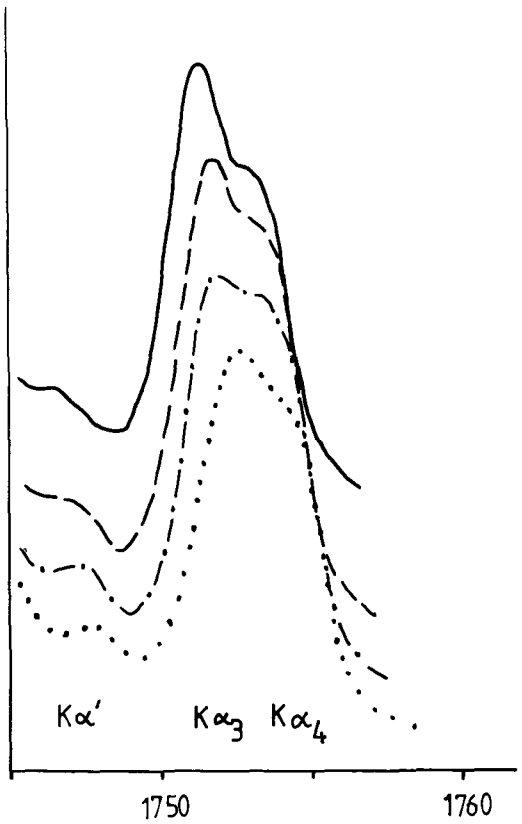

FIG. 7. XE high energy satellite spectra ($K\alpha'$, $K\alpha_3$ and $K\alpha_4$) for various compounds of silicon: SiC, solid line; Si_3N_4, dashed line; SiO_2, dash–dot line; $[SiF_6]^{2-}$ dotted line.

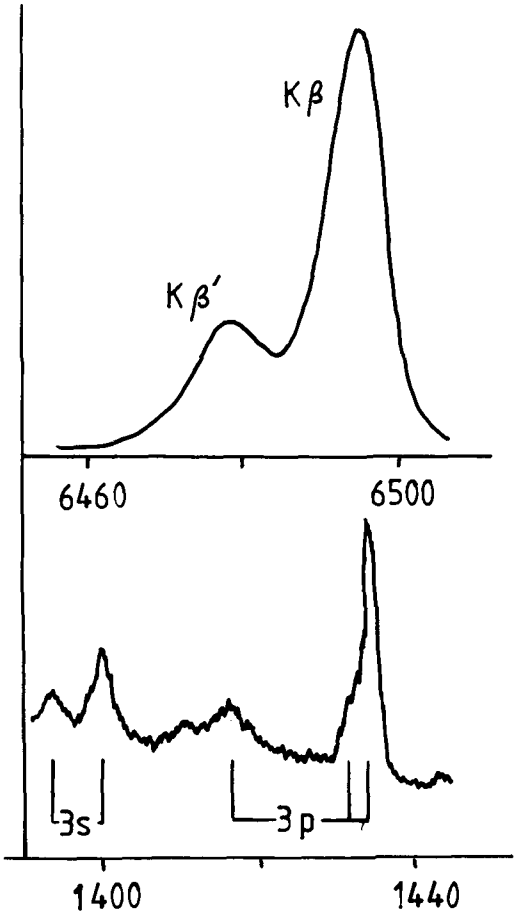

FIG. 8. XE and XP spectra from manganese(II) fluoride. Upper section, Mn–$K\beta$, $K\beta'$ XE spectrum. Lower section, XP spectrum in the Mn 3*s*–3*p* region showing the spin–orbit splitting (energy scale is photoelectron kinetic energy).

coupling between the spin state of the cation and the ionized states associated with XE and XP spectra cause splitting of initial and final energy states. In the case of the high-spin divalent manganese ion, for example (Fadley, 1972), the $3p^{-1}$ state reveals three main components in the XP spectrum (^7P, $^5P_3$ and $^5P_1$–$^5P_2$ is very weak). If such a state is the final state in X-ray emission, then the corresponding XE peak will also show (resolution permitting) the same structure. Fig. 8 shows these effects in XP and XE spectra for MnF_2. In some transition metal compounds, the intensity of $K\beta'$ relative to $K\beta$ can be related to the number of unpaired *d* electrons and thus to valency (Urch and Wood, 1978). Fig. 9 shows how the $K\beta$–$K\beta'$ feature changes with valency for a series of manganese minerals. Similar effects have been observed for Ti (Jones and Urch, 1983) and Cr (Arber *et al.*, 1988) and exploited to determine valency.

Future developments—conclusions

Anisotropy of XE and XP spectra. The spectra discussed above have come from powdered samples from which isotropic emission of photons and electrons could be assumed. But from single crystals, anisotropic emission must be expected. The orbitals involved in the emission of a specific photon or electron will have a specific orientation in space and this orientation will control the electric vector either of the radiation absorbed before the ejection of a photoelectron or of the X-ray as it is emitted (Wiech, 1981). An example of this effect is shown for the XE spectra of calcite in Fig. 10 where it has proved possible to distinguish the σ and π orbitals of the carbonate anion.

Surface studies. Another area where the

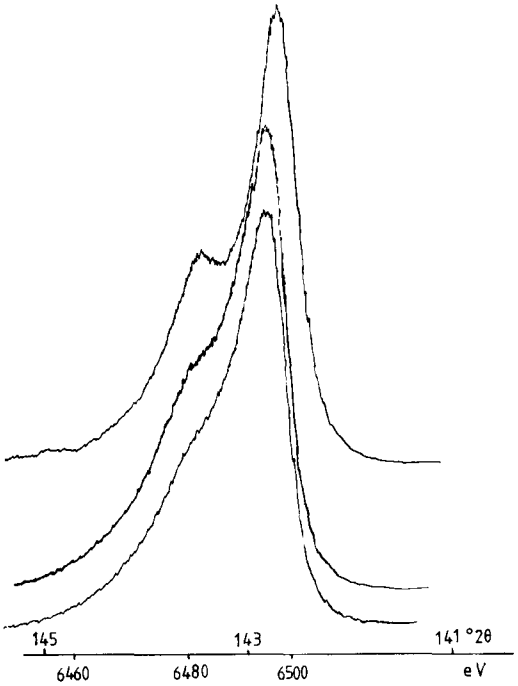

FIG. 9. Mn $K\beta$–β' spectra from manganese in different valency states: upper trace, rhodochrosite–Mn(II); middle trace, manganite–Mn(III); lower trace, pyrolusite–Mn(IV).

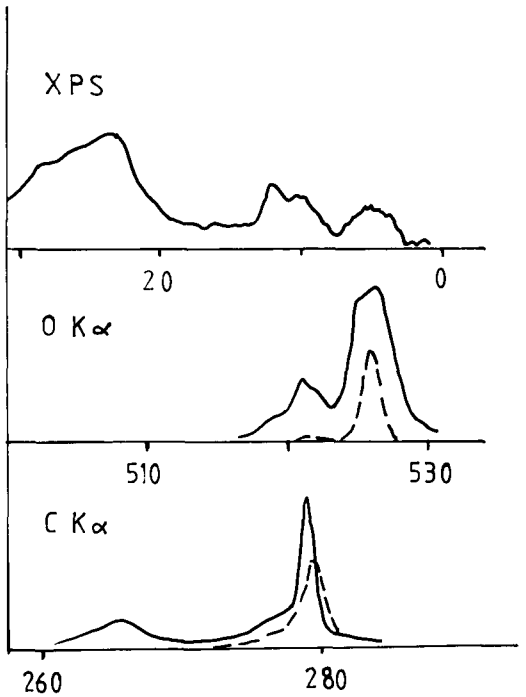

FIG. 10. PAX spectra from a single crystal of calcite. Spectra with different contributions from σ and π character can be collected by varying the take-off angle. The results are shown in the figure. In the lower two traces, X-rays from transitions involving σ orbitals are shown as solid lines, X-rays from π orbitals as dashed lines (data taken from Tegeler *et al.*, 1980).

potential of PAX spectroscopy can be exploited is in the field of Surface Science. XP and Auger spectroscopy, which both monitor the top five to ten atomic layers (1–2 nm), can be complimented by soft X-ray spectroscopy when the spectra are produced by low-energy electron bombardment. If the electron energy is varied then non-destructive depth profiling of surface layers is possible (Romand *et al.*, 1987; Szász *et al.*, 1984). The chemical information carried by the XE spectra enables the chemical state of each element to be determined as a function of depth as well. This method should have considerable application to the investigation of chemical changes at mineral surfaces.

Conclusions. The discussion presented above has shown that the fine structure of XE and XP spectra that involve the valence band can be understood (for the most part) by a simple molecular orbital model and thus used to determine electronic structure.

References

Agarwal, B. K. (1979) X-ray Spectroscopy—An Introduction, Springer-Verlag, Heidelberg, FRG.

Al-Kadier, M. A., Tolon, C. and Urch, D. S. (1984) Photoelectron and X-ray spectroscopy of minerals. Part 1—Electronic structure of forsterite (magnesium orthosilicate). *J. Chem. Soc., Faraday Trans. 2* **80**, 669–79.

Arber, J. M., Urch, D. S. and West, N. G. (1988) Determination of chromium oxidation state by X-ray fluorescence spectrometry: application to chromium (VI) and chromium (III) determination in occupational hygiene samples. *The Analyst* **113**, 779–82.

Atkins, P. W. (1983) *Molecular Quantum Mechanics*, Chapter 10, 2nd ed. Oxford Univ. Press, Oxford, UK.

Berg, U., Dräger, G., Mosebach, K. and Brümmer, O. (1976) Combined XS ND XPS investigations of the FeS_2 valence band. *Phys. Stat. Sol. (b)* **75**, K89–92.

Briggs, D. and Seah, M. P. (1983) *Practical Surface Analysis by Auger and X-ray Photoelectron Spectroscopy*. John Wiley & Sons, Chichester, UK.

Brytov, I. A., Dikov, Yu. P., Romashchenko, Yu. N., Dolin, S. P. and Debol'skii, E. I. (1976) X-ray spectral study of silicate and aluminosilicate minerals. *Izv. Akad. Nauk. USSR, Ser. Fiz.* **40**, 413–19 (Russ.

original), **40** (part 2), 164–9 (Eng. trans.).
Cade, P. E. (1967) Hatree-Fock wavefunctions, potential curves and molecular properties for OH^- ($^1\Sigma^+$) and SH^- ($^1\Sigma^+$). *J. Chem. Phys.* **47**, 2390–406.
Collins, G. A. D., Cruickshank, D. W. J. and Breeze, A. (1972). *Ab Initio* calculations on the silicate ion, orthosilicic acid and their $L_{2,3}$ X-ray spectra. *J. Chem. Soc., Faraday Trans. II* **68**, 1189–95.
Compton, A. H. and Allinson, S. K. (1935) *X-rays in Theory and Experiment.* Van Nostrand, New York, NY, USA.
Dikov, Yu., P., Debolsky, E. I., Romashchenko, Yu. N., Dolin, S. P. and Levin, A. A. (1977) Molecular orbitals of $Si_2O_7^{6-}$, $Si_3O_{10}^{8-}$ etc. and mixed (B, Al, P, Si)$_m$ applied to clusters and X-ray spectroscopy data of silicates. *Phys. Chem. Minerals* **1**, 27–41.
Dodd, C. B. and Glenn, G. L. (1968*a*) Chemical bonding studies of silicates and oxides by X-ray K-emission spectroscopy. *J. Appl. Phys.* **39**, 5377–84.
——— (1968*b*) A survey of the chemical bonding in silicate minerals by X-ray emission spectroscopy. *Am. Mineral.* **54**, 1299–311.
Domcke, W., Cederbaum, L. S., Schirmer, J., von Nieesen, W. and Maier, J. P. (1978) Breakdown of the molecular orbital picture of ionization for inner valence electrons: experimental and theoretical study of H_2S and PH_3. *J. Elec. Spec. and Rel. Phenom.* **14**, 59–72.
Fadley, C. S. (1972) Multiplet splittings in photoelectron spectra. In *Electron Spectroscopy.* (Shirley, D. A., ed.), North-Holland Pub. Co., Amsterdam, Netherlands, pp. 781–801.
Fischer, D. W. and Baun, W. L. (1965) Diagram and nondiagram lines in the K spectra of aluminium and oxygen from metallic and anodized aluminium. *J. Appl. Phys.* **36**, 534–7.
Frost, D. C., Ishitani, A. and McDowell, C. A. (1972) X-ray photoelectron spectroscopy of copper compounds. *Molec. Phys.* **24**, 861–77.
Glenn, G. L. and Dodd, C. G. (1968) Use of molecular orbital theory to interpret X-ray K-absorption spectra data. *J. Appl. Phys.* **39**, 5372–7.
Hagström, S. B. M. and Fadley, C. S. (1974) X-ray photoelectron spectroscopy. In *X-ray Spectroscopy.* (Azaroff, L. V., ed.), McGraw Hill, New York, NY, USA, pp. 379–444.
Haycock, D. E., Kasrai, M., Nicholls, C. J. and Urch, D. S. (1979) The electronic structure of magnesium hydroxide (Brucite) using X-ray emission, X-ray photoelectron and Auger spectroscopy. *J. Chem. Soc.—Dalton Trans.*, pp. 1791–6.
Herglotz, H. K. and Birks, L. S. (1978) *X-ray Spectrometry.* Marcel Dekker, New York, NY, USA.
Holm, R. and Storp, S. (1977) ESCA studies on changes in surface composition under ion bombardment. *Appl. Phys.* **12**, 101–12.
Jenkins, R. and de Vries, J. L. (1970) *Practical X-ray Spectrometry.* MacMillan, London, UK.
Jones, J. B. and Urch, D. S. (1983) Analytical potential of valence state and ligand atom effects in titianium K X-ray spectra. *The Analyst* **108**, 1477–80.
Krause, M. O. and Carlson, T. A. (1967) Vacancy cascade in the reorganization of krypton ionized in an inner shell. *Phys. Rev.* **158**, 18–24.
Larkins, F. P. and Rowlands, T. W. (1986) Importance of Interatomic Contributions to Molecular X-ray Emission Processes. *J. Phys. B: Atomic and Mol. Phys.* **19**, 591–7.
Läuger, K. (1972) Über den Einfluss der Bindungsart und der Kristall-struktur auf die Röntgen $K\alpha$-satelliten von Aluminium. *J. Phys. Chem. Solids* **33**, 1343–53.
Li, E. K., Johnson, K. H., Easman, D. E. and Freeouf, J. L. (1974) Localized and band valence–electron states in FeS_2 and NiS_2. *Phys. Rev. Letters* **32**, 470–2.
Manne, R. (1970) Interpretation of X-ray Emission Spectra of Molecules. *J. de Physique* **32–C4**, 151–3.
Martin, R. L. and Shirley, D. A. (1977) Many electron theory of electron emission. In *Electron Spectroscopy: Theory, Techniques and Applications* **1** (Brundle, C. R. and Baker, A. D., eds.). Academic Press, London, UK, pp. 75–117.
Murrell, J. N., Kettle, S. F. A. and Tedder, J. M. (1965) *Valence Theory.* John Wiley & Sons, London, UK.
Price, W. C. (1977) Ultraviolet photoelectron spectroscopy: basic concepts and the spectra of small molecules. In *Electron Spectroscopy: Theory, Techniques and Applications* **1** (Brundle, C. R. and Baker, A. D., eds.). Academic Press, London, UK, pp. 151–203.
Purton, J. A. and Urch, D. S. (1989) High resolution silicon $K\beta$ spectra and crystal structure. *Mineral Mag.* **53**, 239–44.
Rivière, J. C. (1983) Instrumentation. In *Practical Surface Analysis* (Briggs, D. and Seah, M. P., eds.). John Wiley & Sons, Chichester, UK, pp. 17–85.
Romand, M., Bador, R., Charbonnier, M. and Gaillard, F. (1987) Surface and near-surface chemical characterization by low-energy electron induced X-ray spectrometry (LEEIXS), a review. *X-ray Spectrometry* **16**, 7–16.
Scofield, J. H. (1976) Hartree-Slater subshell photoionization cross-sections at 1254 and 1487 eV. *J. Electr. Spec. and Rel. Phenom.* **8**, 129–37.
Siegbahn, K., Nordling, C., Johansson, G., Hedam, J., Hedén, P. F., Gelius, U., Bergmark, T., Werme, L. O., Manne, R. and Baer, Y. (1969) *ESCA applied to free molecules.* North-Holland Pub. Co., Amsterdam, Netherlands.
Sugiura, C., Suzuki, I., Kashiwakura, J. and Goshi, Y. (1976) Sulfur $K\beta$ X-ray emission bands and valence-band structures of transition-metal disulfides. *J. Phys. Soc. Japan* **40**, 1720–4.
Szász, A., Kojnok, J. and Kertész, L. (1984) Soft X-ray depth analysis (SXDA) as a new tool for interface spectroscopy. Abstracts, *Int. Conf. on X-ray and Inner-shell processes in atoms, molecules and solids.* (Meisel, A., ed.). Karl-Marx-Univ., Leipzig, DDR, pp. 455–7.
Taniguchi, K. and Henke, B. L. (1976) Sulfur $L_{11,111}$ emission spectra and molecular orbital studies of sulfur compounds. *J. Chem. Phys.* **64**, 3021–35.
Tegeler, E., Kosuch, N., Wiech, G. and Faessler, A. (1980) Molecular orbital analysis of the CO_3^{--} ion

by studies of the anisotropic X-ray emission of its components. *J. Elect. Spec. and Rel. Phenom.* **18**, 23–8.

Tossell, J. A. (1973) Molecular orbital interpretation of X-ray emission and ESCA spectral shifts in silicates. *J. Phys. Chem. Solids* **34**, 307–19.

——(1975) The electronic structures of silicon, aluminium and magnesium in tetrahedral coordination with oxygen from SCF–$K\alpha$ MO calculations. *J. Am. Chem. Soc.* **97**, 4840–4.

——(1977) A comparison of silicon–oxygen bonding in quartz and magnesium olivine from X-ray spectra and molecular orbital calculations. *Am. Mineral.* **62**, 136–41.

——Vaughan, D. J. and Johnson, K. H. (1973) X-ray photoelectron, X-ray emission and UV spectra of SiO_2 calculated by the SCF $X\alpha$ scattered wave method. *Chem. Phys. Letters* **20**, 329–34.

Urch, D. S. (1969) Direct evidence for $3d$–$2p$ π-bonding in oxy-anions. *J. Chem. Soc. A* pp. 3026–8.

——(1970) The origin and intensities of low energy satellite lines in X-ray emission spectra: a molecular orbital interpretation, *J. Phys. C: Solid State Phys.* **3**, 1275–91.

——(1979) *Orbitals and Symmetry*, Macmillan, Basingstoke, UK.

——(1982) The temporary covalence of potassium fluoride (in X-ray and Auger spectra processes). *J. Chem. Soc.—Chem. Comm.* pp. 526–8.

——(1985) X-ray spectroscopy and chemical bonding in minerals. In *Chemical Bonding and Spectroscopy in Mineral Chemistry* (Berry, F. J. and Vaughan, D. J., eds.). Chapman and Hall, London, UK, pp. 31–61.

——and Wood, P. R. (1978) The determination of the valency of manganese in minerals by X-ray fluorescence spectroscopy. *X-ray Spectroscopy* **7**, 9–11.

White, E. W. and Gibbs, G. V. (1967) Structural and chemical effects on the Si–$K\beta$ X-ray line for silicates. *Am. Mineral.* **52**, 985–93.

Wendin, G. and Ohno, M. (1976) Strong dynamical effects of many electron interactions in photoelectron spectra from 4s and 4p core levels. *Physica Scipta* **14**, 148–61.

Wiech, G. (1981) *Anisotropic emission of radiation, in inner shell and X-ray physics of atoms and solids.* (Fabian, D. J., Kleinpoppen, H. and Watson, L. M., eds.), Plenum Press, London, UK, pp. 815–23.

——Köppen, W. and Urch, D. S. (1972) X-ray emission spectra and electronic structure of the disulphide anion. *Inorg. Chim. Acta* **6**, 376–8.

[*Manuscript received 3 May 1988: revised 29 July 1988*]